 CMC, vol.1, no.4, pp.309-318, 2004

Plasma Etching to Enhance Visibility of Nano Particles in Nanocomposites

Kunigal N.Shivakumar[1], Shivalingappa Lingaiah[2], Robert Sadler[2], Matthew Sharpe[2]

Abstract: The exfoliation and dispersion of nanoclay (2% by weight) and nanovermiculite (2% by weight) particles in a polymer matrix is analyzed using the Scanning Electron Microscope (SEM) after a low temperature air plasma etch. The plasma etch preferentially removes the polymer to expose the nanoparticles. Both Argon and air have been used as the etching media to study the etching process. SEM analysis illustrate the results of the etching in flat and edge surfaces of both nanoclay (MMT) and nanovermiculite (VMT) filled polymer. Both the MMT and VMT were dispersed using a IKA high shear mixer and a Sonicator.

keyword: Nanoclay, nanovermiculite, plasma etching, SEM

1 Introduction

Adding a small quantity of nanoparticles to certain polymers has been found to be useful in modifying the properties required for some specific applications. One class of materials such as, MMT/ polymer materials have displayed remarkable increase in the mechanical properties per unit weight of the reinforcing additive [Yoshihara, Oie, Okada, Matsui, and Ohshiro (2002), Tamaki, Choi, and Laine (2003), Pyun, Matyjaszewski, Kowalewski, Savin, Patternson, Kickelbick, and Huesing (2001), Li, Wang, Toghiani, Daoulton, Koyama, and Pittman (2001), He, Valluzzi, Yang, Dolukhanyan, Sung, Kumar, Tripathy, Samuelson, Balogh, and Tomalia (1999), Percy, Barthet, Lobb, Khan, Lascelles, Vamvakaki, and Armes (2000), Patton, Pittman, Wang, and Hill (1999), Lan and Pinnavaia (1994), Manias (2001), Herman and Boenig (1988)]. As an example, a small amount of MMT added to a phenolic molding compound has been found to reduce the erosion rate in a rocket nozzle application [Koo, Stretz, Bray, Wootan, Mulich, Powell, Weispfenning, and Grupa (2003)]. In order to obtain superior performance in nanocomposites it is important to achieve extensive exfoliation and dispersion of MMT in the polymer. This can be achieve by a number of mixing techniques, all involving high shear. The primary technique to determine the extent of exfoliation and dispersion is the Transmission Electron Microscopy (TEM) [Mitra, Hossein, Kingery, and Pittman (2004)]. Using this technique exfoliation and dispersion can be seen. The limitation of this technique is the small area of visualization and the sample size observed may not be representative of the whole. In addition, the procedure requires replica preparation of surface to be visualized, which is quite tedius. Furthermore the equipment required is not widely available. In addition to the TEM measurements, X-ray Diffraction (XRD) [Mitra, Hossein, Kingery, and Pittman (2004, Morgan, Gilman, and Jackson (2000), Gilman and Morgan (2003)] are being used for computing the 'd' spacing in the cured nanocomposites. The Small-Angle X-ray Scattering (SAXS) are being used to study the exfoliation process by some investigators [Mitra, Hossein, Kingery, and Pittman (2004]. Here the sample to detector distance is very large about (1.1 meters) for a 20 sq. cms detector area. Corrections are needed for instrumental dark current due to cosmic radiation and electronic noises in the detector circuitry. The high resolution TEM and Small-angle neutron scattering (SANS) are also being used for computing the exfoliation of nanoclay platelets by other investigators [Glinka (2002), Ho, Briber, and Glinka (2001)]. These are very expensive techniques for computing exfoliation and dispersion of nanoplatelets. All these techniques are not simple enough to be adopted for manufacture process development.

As new composites based on nanotechnology are developed and characterized for various applications, the subject of quality control in a manufacturing process becomes an important issue. To obtain dependable properties, the degree of exfoliation as well as dispersion must be easily determined. As explained previously, TEM,

[1] Research Professor and Director, Center for Composite Materials Research, Department of Mechanical Engineering, North Carolina A&T State University, Greensboro, NC 27411

[2] Center for Composite Materials Research, North Carolina A&T State University, Greensboro, NC 27411

XRD, SAXS, SANS have limited user applicability. This paper explains the plasma etch followed by SEM examination as an abbreviated technique for this determination of exfoliation/dispersion in nanocomposites.

Objective of this paper is to demonstrate how a low temperature plasma etching followed by SEM examination can be used to assess the degree of exfoliation and dispersion of nano platelets in a polymer composite.

The following section describes the plasma etching technique and its applications for etching different materials. Preparation of nanocomposite samples of MMT and VMT, plasma etching process, SEM studies and their results are presented.

2 Plasma Etching Technique

Plasma etching is a chemical process where RF discharge is used to generate reactive species such as atoms, free radicals and ions from parent gases. The discharge is stuck in a vacuum chamber containing the substrates to be etched and the reactive species diffuse into the substrate surface where they react to form volatile compounds. These compounds are escape from the surface and finally are pumped out by the vacuum pump.

2.1 Advantages of Plasma Etching

1. Plasma activity is uniform across the electrode surface, thereby creating a uniform etch profile for processing of three dimensional objects
2. Results are controllable and repeatable
3. Surface treatment of individual parts is independent of location and orientation on the electrodes.

2.2 Application of Plasma Etching

Plasma etching is widely used in the electronic industry particularly for microelectronic fabrication such as multi step processing of complex devices [Bersin (1978)], photo resist removal [Inving (1968)], etching silicon compounds [Abe, Sonbe, and Enomoto (1973)], etc. The major application of plasma etching is in ion milling. Ion milling or ion beam etching involves no chemical reactions since it uses noble gases like argon. This process is operated at low pressures below 10^{-3} torr. Plasma etching is used in etching of different materials such as silicon, silicon dioxide, silicon nitrate. It is also used in the etching of $SrBi_2Ta_2O_9$ thin films in a $Cl_2/CF_4/Ar$ plasma [Kim and Kim (2002)], dry etching of GaAs, removal of polysilicon films [Christopher, Himmel, and May (1993)]. Argon plasma sputter-etched induced defects in strained, epitaxial p-type Si-Ge layers were studied by other investigators [Marnor, Auret, Goodman, and Malherbe (1999)]. Plasma etching was also used for the fabrication of lithographic masks for the production of nanosized surface features [Kim, Yang, Boo, and Han (2003), Hanarp et al (2003)] and for different applications.

Low temperature plasma processing is widely used in the preparation of micro chips. It is also used for other etching and cleaning process in manufacturing plants. The low temperature plasma is based on ionizing a gas at low pressure in an RF field. Each gas has a particular color and chemical activity. As the additional power is applied to the RF field, the ionized particles become more aggressive. It has been said that a plasma of Argon is equivalent to sand blasting at an atomic level.

3 Experimental Procedure

This section includes the preparation of MMT and VMT nanocomposite samples and plasma etching of these samples at different etching conditions. The details are given below:

3.1 Preparation of nanocomposite samples

3.1.1 MMT nanocomposite

The MMT samples were prepared by mixing 150 grams of Derakane 510A-40 epoxy vinyl ester resin (VE) [The Dow Chemical Co.] with 3 grams (2% by weight) of Cloisite 10A (Southern Clay, Gonzales, TX). The MMT was dispersed in the VE using an IKA Turrax T-18 mixer with a 19 mm mixing shaft set at about 6,000 rpm. The mixing was accomplished by three 10 minutes mixing cycles with a cooling period between each cycle. The mechanical action of the mixer heated the mixture and the cooling cycle was introduced to keep the VE from overheating and thus reducing the styrene monomer content of the VE which is approximately 35% styrene monomer.

The MMT/VE mixture was then catalyzed using 0.3% Cobalt Naphthenate (6%) promoter, 0.75% cumene hydroperoxide catalyst and 0.075% 2,4-pentanedione retarder. Each ingredient was weighed and hand-stirred into the MMT/VE mixture before the next ingredient is

added. It was observed that the MMT had an accelerating effect on the VE gel time. The addition of more retarder as shown in the above formulation provided sufficient pot-life for the casting process. The catalyzed mixture was degassed in a vacuum chamber to remove the entrapped air. Degassing was difficult because the foam refuses to collapse because of the MMT addition. However much of the air was removed by the degassing process. The catalyzed mixture was cast into a sheet and cured at room temperature for about 72 hours. The material was then post cured for 8 hours at 82°C.

3.1.2 VMT nanocomposite

The VMT used for these experiments was prepared from Palmetto's medium A-2 vermiculite aggregate. Each sample contains five grams of this VMT was disaggregated in 1,000 mls of deionized water using a high shear IKA mixer at 24,000 rpm for 15 minutes. The suspension was centrifuged by settlement using a transfer pipette and then the centrifuge turned at 4,000 rpm and was run for 10 minutes. The material remaining in suspension and that separated by the centrifuge were examined by using inductively coupled plasma-optical emission spectroscopy (ICP-OES). The analysis was performed on the 0.25 ml of digested residues and/or VMT mixed with 7ml of saturated boric acid solution. The digestion process was carried out by adding 0.2 gram of VMT to a concentrated mixture of acids (10ml HF+4ml HCl+1 ml HNO_3). The elemental analysis of VMT was Al=11.42, K=145.53, Ca=24.08, Fe=13.85, Mg=398.44 ppm. The material remaining in suspension was considered to be nanosized VMT and stored in deionized water. The material that was thrown out by the centrifuge was analyzed and found to contain 1139 ppm K per gram. The thrown out material was considered to be mica and discarded. This water suspension contain 5 gram of VMT was then washed with HCl (pH - 5) three times for one hour for each time. The acid treated VMT was concentrated by centrifuge and stored in deionized water. The cation exchange capacity (CEC) was determined by the titration with NaOH to a phenolphthalein end point resulting in a CEC value of 100 meq/100 grams. The VMT was then intercalated using 5 meq of cetyl tri methyl ammonium bromide (CTMA) dissolved in 500 ml of deionized water. The mixture was then stirred for 24 hours at 70-80°C. Then 200 ml of the mixture was sonicated for 5 minutes while being circulated by a magnetic stirrer. This was then dried in an oven at 80°C for 24 hours. Two percent of the dried intercalated VMT was then added to the Derakane 510A-40 VE.

The VMT/VE mixture was dispersed using the IKA high shear mixer at 10,000 rpm for two minutes. The mixing container was position in a 25°C water bath to provide some cooling. After the two minutes of mixing, the container was allowed to cool for 30 minutes after which the viscosity was measured. The mixing/cooling process was repeated for about 12 minutes at which time the viscosity stabilized. The mixture was then catalyzed using 0.3% Cobalt 2-Ethylhexanoic (6%) promoter, 1.25% Trigonox 239A catalyst and 0.1% 2,4-pentanedione retarder. Each ingredient was weighed and hand-stirred into the VMT/VE mixture before the next ingredient is added. The catalyzed mixture was then degassed in a vacuum and cast into a sheet. The sheet was cured for about 72 hours at room temperature and then post cured for 8 hours at 82°C.

3.2 Plasma etching of samples

Samples of cured MMT/VE and VMT/VE nanocomposites were exposed to the ionized gas in the low temperature plasma chamber. The sample size was about 5x5 mm. The thickness was a variable depending how the composite was casted. The plasma machine utilized was a Branson/IPC, model number P210073. The front view of the etching system is shown in figure 1. Figure 2 illustrates a view of the etching system with the door open.

The chamber consist of a quartz tube about 250 mm in diameter and 450 mm deep. A schematic of the plasma machine is illustrated in figure 3. The samples were placed on a perforated aluminum tray that positioned the samples about midway in the plasma chamber. The RF power is turned on to warm-up the electronic system. The chamber is evacuated to about 0.001 torr and the dry air is allowed to flow slowly into the chamber. After the gas pressure stabilized the RF power was increased to the level indicated in Tables 1 and 2. The initial glow of the plasma was at about 150 watts. Additional power was used to obtain a uniform glow that was confined to the chamber. The uniform glow in the plasma chamber is shown in figure 4. Care must be exercised to limit the RF power to prevent the plasma glow from flowing into the vacuum plumbing.

The first set of samples were etched in an Argon plasma.

Figure 1 : Front view of etching system

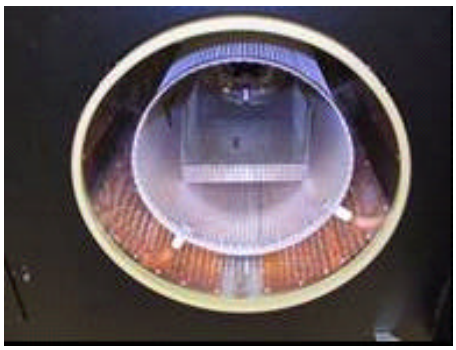

Figure 2 : Inside view of etching chamber

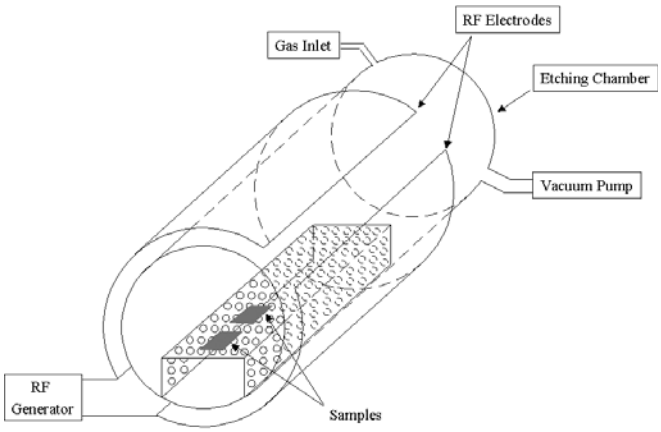

Figure 3 : A schematic of plasma etching system

Figure 4 : Plasma glow in etching system

Table 1 : Samples Etched with an Argon Plasma

Run Number	Etching Time (Minutes)	Gas Pressure (Torr)	RF Power (Watts)
1	51	0.25	165
2	139	0.25	165

Argon gas was selected because it is chemically inert and has a relatively high mass. The conditions of the Argon etch are shown in Table 1 below.

The plasma chamber temperature increased during the etching process using Argon. The etching of the samples was carried out in step sequence because the maximum operating temperature of the chamber is 70°C. In argon etching, the initial temperature was 31°C and increased to 61°C in 24 minutes of etching period. When the chamber temperature was increased to 61°C, the etching process was stopped and allowed the chamber to cool for 45 minutes until the temperature stabilized to about 31°C. The step sequence of etching is repeated till the required etching period was met. Although samples were etched for 2 duration etching, only the result of 139 minutes etching are presented.

The next set of samples were etched in an air plasma. The

Table 2 : Samples Etched with a Dry Air Plasma

Run Number	Etching Time (Minutes)	Gas Pressure (Torr)	RF Power (Watts)
1	16	0.30	250
2	32	0.30	250
3	50	0.30	250
4	90	0.30	250

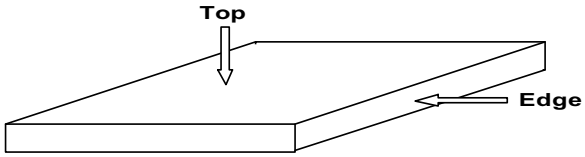

Figure 5 : The top and edge views of SEM imaging

active ingredient in air is Oxygen. Prior experience has taught that the use of pure Oxygen results in very rapid etching causing repeatability problems. A drying tube was used to remove the moisture contained within the room air. The Argon etching etches while the Oxygen plasma primarily etches by oxidation of polymer thereby exposing the mineral nanoparticles. The nano mineral filler remains unaffected by the plasma under these conditions used.

The temperature in the plasma chamber also increased during the etching treatment with dry air. This time the chamber temperature increased from an initial temperature of 32^{o}C to 63^{o}C in 8 minutes. A stepped heating and cooling sequence was used here also as explained in argon plasma etching.

After the plasma etching, the samples were coated with gold using sputtering system to improve the conductivity of the surface for SEM study. The samples were imaged in SEM (Hitachi S-3000N) at different magnifications to assess the dispersion and exfoliation at microscopic and nanoscopic levels. The top and edge views of the samples were taken as illustrated in figure 5. These two views could reveal the preferential orientation of nanoplates caused by the coating technique. Although samples were etched for 4 duration etching, only the results of 50 and 90 minutes etching are presented.

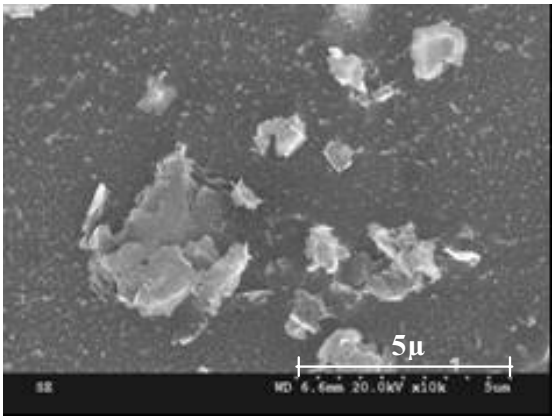

a. MMT/VE nanocomposite

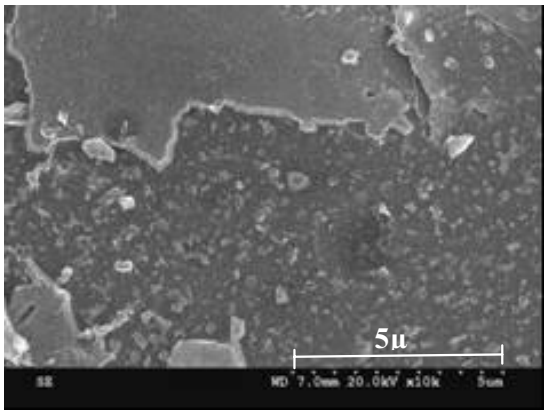

b. VMT/VE nanocomposite

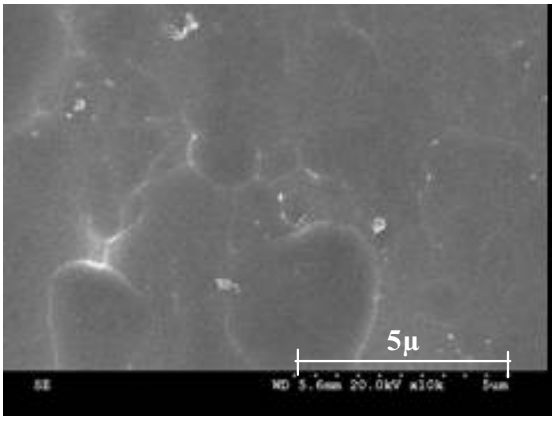

c. Unfilled VE

Figure 6 : SEM images of MMT/VE, VMT/VE and VE nanocomposite at x10k magnification.

4 Results and Discussion

4.1 Argon plasma etched nanocomposites

The Figure 6 shows the SEM images of argon plasma etched nanocomposite and VE samples for 32 minutes at

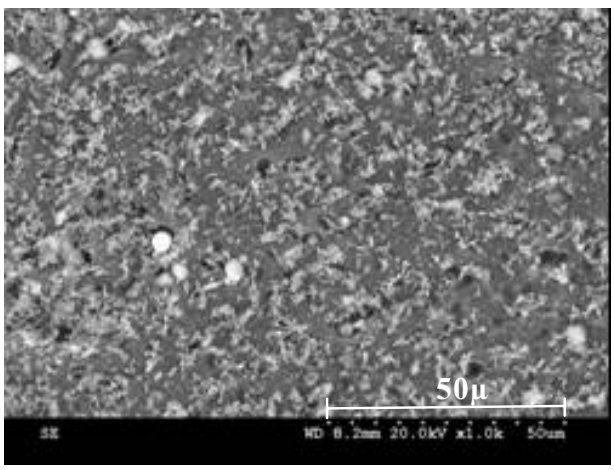

a. x1k

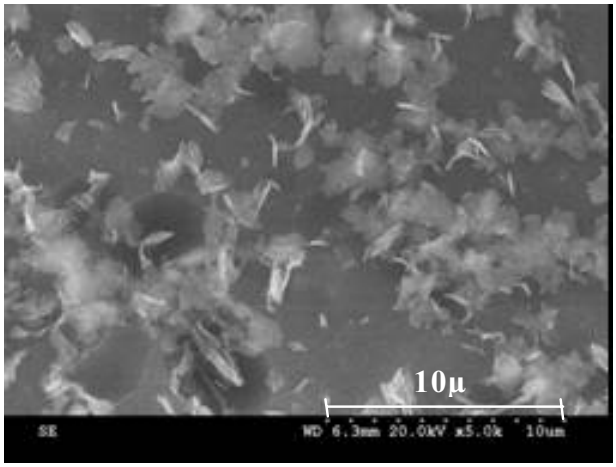

b. x5k

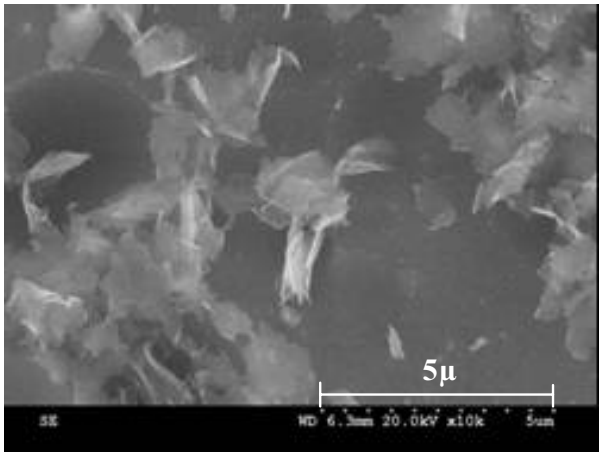

c. x10k

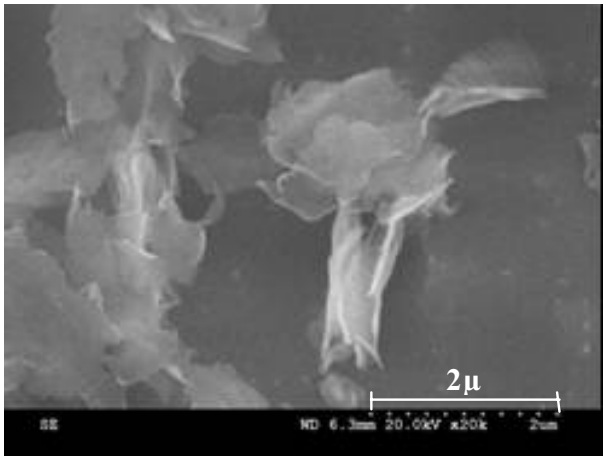

d. x20k

Figure 7 : SEM top views of MMT/VE nanocomposite at different magnifications

10k magnification. The large particles shown in Figure 6 (a) are about the same size as the MMT provided by the supplier. The smaller particles in the background are nanosized MMT particles that are uniformly dispersed. Figure 6(b) clearly illustrates some of the VMT pictures of larger size or not exfoliated VMT but the background is populated with smaller particles. The back particles may be uniformly dispersed nanoplatelets or deposition of eroded material. This need to be investigated further. Figure 6(c) shows the plasma etched VE matrix under the same magnification. Note the absence of the nano particles.

4.2 Air plasma etched MMT/VE nanocomposites at different magnification

Figure 7(a) through 7(d) shows air plasma etched MMT/VE nanocomposites for 50 minutes at 1k, 5k, 10k and 20k magnifications respectively. Images were of the top surface of the sample. Figure 7(a) is a clearly illustrates a uniform dispersion of micron size particles or we conclude that the material is microscopically homogeneous. Figure 7(b) illustrates the dispersion of micro size particles. Figure 7(c) clearly illustrates the exfoliation of nanoclay into platelets of varying degree. It also shows the platelets have curved surfaces indicating various stages of exfoliation. Figure 7(d) further shows more

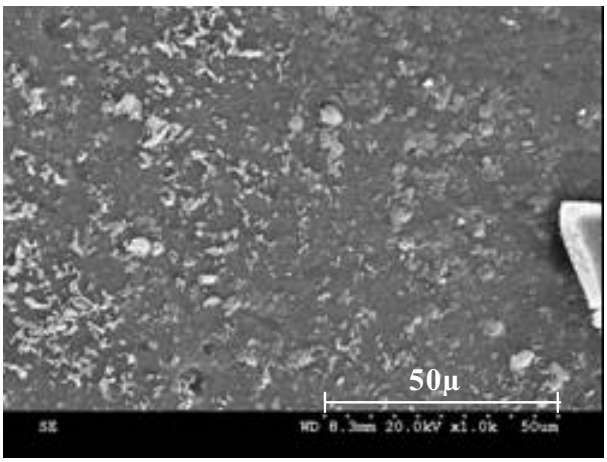

a. x1k

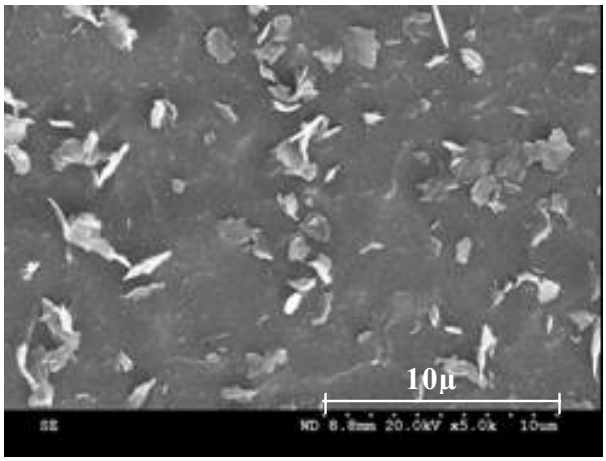

b. x5k

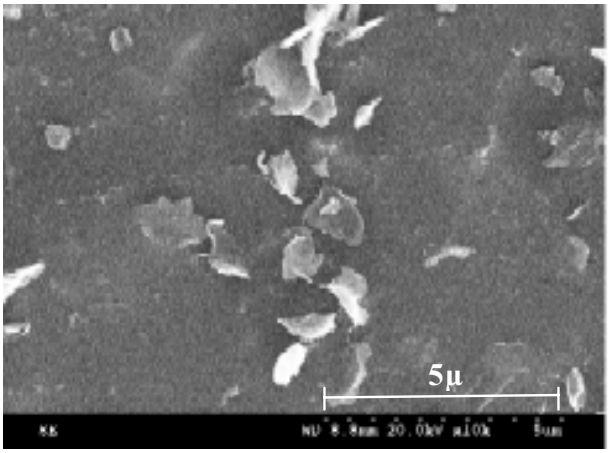

c. x10k

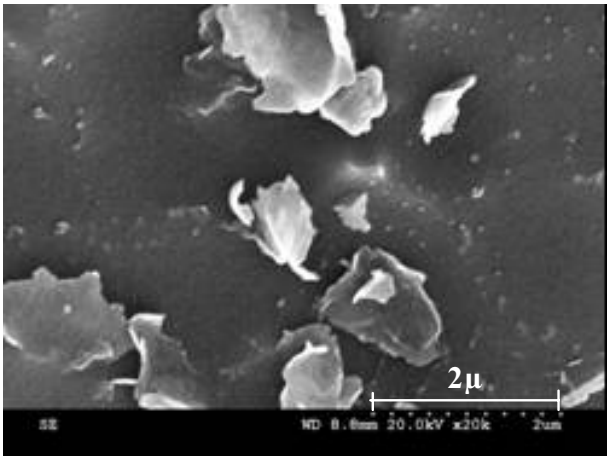

d. x20k

Figure 8 : SEM edge views of MMT/VE nanocomposite at different magnifications

details of exfoliation MMT. Also, these figures illustrates the incomplete exfoliation and dispersion of MMT in the polymer. More shearing is needed to achieve more complete exfoliation and dispersion.

4.3 Air plasma etched on edge surface of the MMT/VE nanocomposite

SEM pictures of the edges of the sample after 50 minutes of air plasma etched are shown in figure 8(a) through 8(d). Figure 8(a) looks like Figure 8(b) and further confirms a microscopic uniformity of the particles. Figure 8(c) illustrates the uniform dispersion on micron size particles. Figure 8(d) again illustrates some level of exfoliation.

4.4 Air plasma etched on top and edge surface of MMT/VE nanocomposite

Figures 9(a) and 9(b) shows top and edge surface views of nanocomposite etched in air plasma for 90 minutes. Both figures shows some level of exfoliation and dispersion. The difference between looking at a top and an edge surfaces of the sample is not significant. Figure 9(c) and 9(d) shows the figures of 9(a) and 9(b) at double the magnification. They show more details of exfoliation. The smaller background particles are not clearly understood. By comparing figures 7 and 9, one can conclude that the background visible particles may be ash from the decomposition of the polymer caused by extended etch-

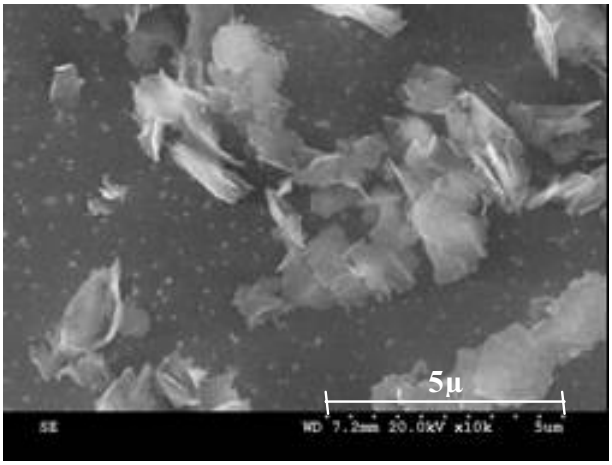

a. Top surface view (x10k)

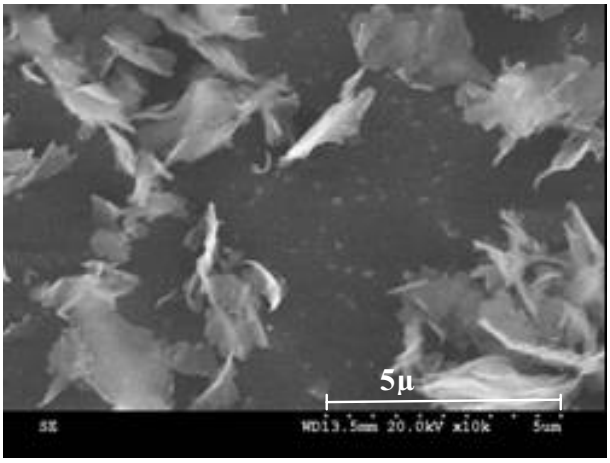

b. Edge surface view (x10k)

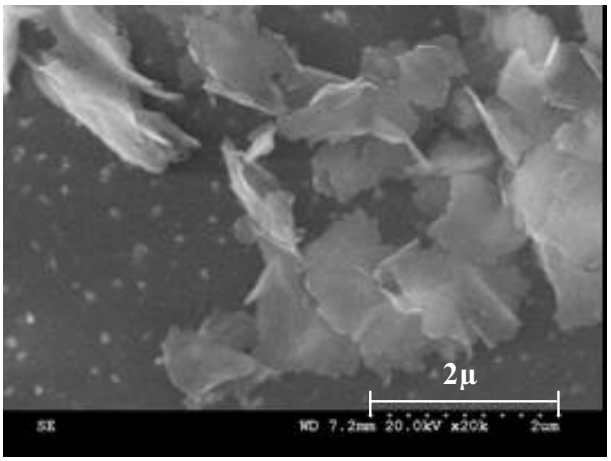

c. Top surface view (x20k)

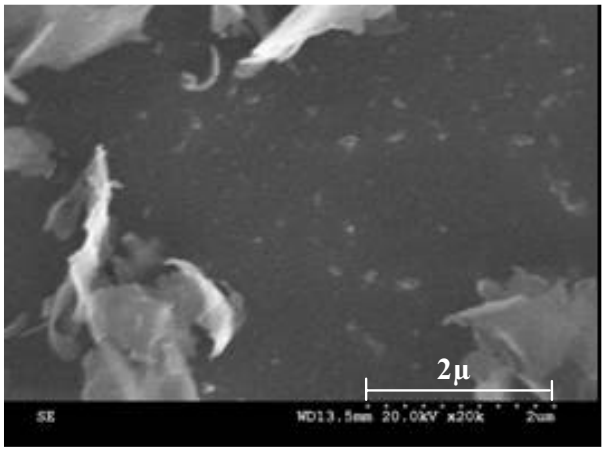

d. Edge surface view (x20k)

Figure 9 : Comparison of top and edge surface views of MMT/VE nanocomposite at x10k and x20k magnifications.

ing. Pictures beyond 20k magnifications started blurring.

4.5 Polymer containing VMT/VE nanocomposite

Figure 10(a) to 10(c) shows top surface SEM images of VMT/VE composite etched in air plasma for 50 minutes. Figure 10(a) has a feature unseen before. There is a cavity in VE surrounding some of the VMT particles. It is believed that the RF field coupled to the iron boundary had increased the particle temperature to accelerated the polymer rate of etching near the particle. Figure 10(b) more clearly illustrates the inner etch depth near VMT particles. Figure 10(c) shows the polymer containing VMT particles at higher magnification. This composite appears to be not properly exfoliated and dispersed.

5 Conclusions

The use of air plasma etch to expose the morphology of nano mineral filled composites followed by SEM imaging is a promising technique for quick evaluation of exfoliation and dispersion of nanofillers. This was studied using nanoclay/vinyl ester and nanovermiculite/vinyl ester nanocomposite samples made at Center for Composite Materials Research, North Carolina A & T State University. This process certainly exposes the uniformity and shape of the larger nanoplatelets as well as gives visi-

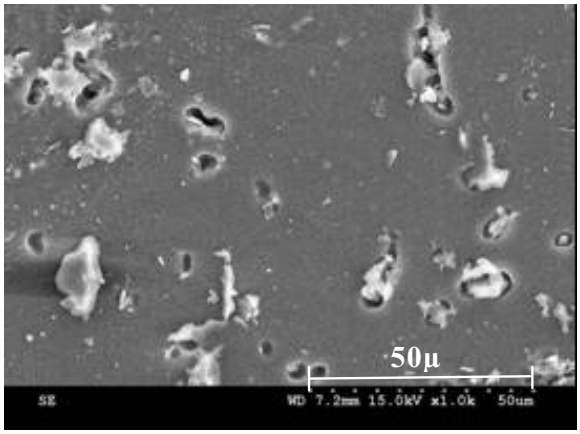

a. x1k

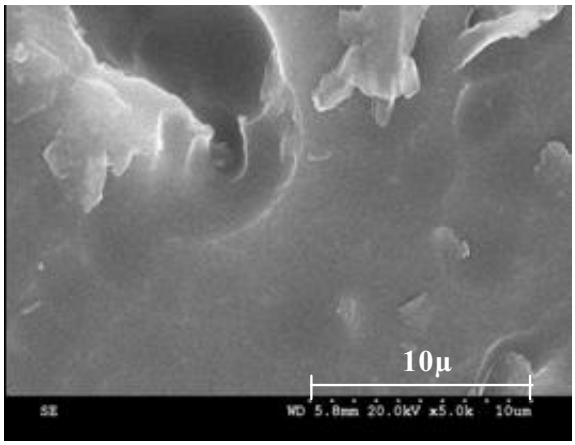

b. x5k

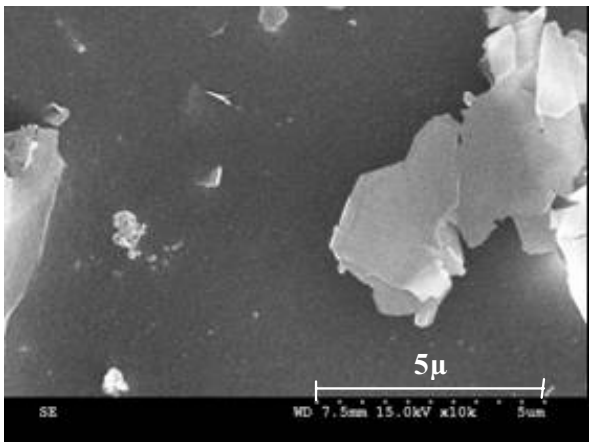

c. x10k

Figure 10 : SEM top views of VMT/VE nanocomposite at different magnification

bility of exfoliation as well as the dispersion. The SEM may not be adequate to determine the level of exfoliation and that may always be in the realm of the TEM. The SEM photo clearly shows some level of exfoliation. The SEM photos are indeed interesting in that a larger area may be studied as well as the exposure of the larger particles to SEM analysis. However, the smaller background particles are not clearly understood. The coupling of the RF field to iron content could be a problem with the VMT/VE nanocomposite from SEM analysis. The SEM has allowed to see smaller to larger areas and reconstruct the 3-D view of the larger area which is not possible from TEM or other technique.

Acknowledgement: The authors wish to thank the Offices of Naval Research for financial support through a grant N 00014-01-1033 and Dr. Yapa Rajapakse, Program Manager for ship structure. The authors also acknowledge Dr. Zhigang Xu, Center for Smart Material and Advanced Structure for his help in analyzing the samples using SEM. They also thank Mr.Patrick Stuart, for his help in preparing the samples.

References

Abe, A.; Sonbe, Y.; Enomoto, T. (1973): *Jpn. J.Appl. Phys.*, Vol. 12, pp. 154.

Bersin, R. L. (1978): Kodak Microelectronics Seminar Proc., San Diego, California, October 1-3.

Christopher, D.; Himmel; May, G. S. (1993): Advantages of Plasma Etch Modeling Using Neural Networks Over Statiscal Techniques, *IEEE Transactions on Semiconductor Manufacturing*, Vol. 6, pp.103-111.

Gilman, J. W.; Morgan, A. B. (2003): Characterization of Polymer-layered silicon (clay) nanocomposite by transmission electron microscope and x-ray diffraction: A comparative study, *J. Appl. Polym. Sci.*, Vol. 87, pp.1329-1338.

Glinka, C. J. (2002): Summer School Notes on Neutron Scattering and Reflectometry from Submicron Structures, NIST, Center for Neutron Research, June 3-7, 2002.

Hanarp; Per.; Sutherland, Gold, D. S.; Julie; Kasemo; Bengt (2003): Control of nanoparticle film structure for colloidal lithography, *Colloids and Surfaces A: Physicochemical and Engineering Aspects*, Vol. 214, n 1-3, pp. 23-36.

He, J. A.; Valluzzi, R.; Yang, K.; Dolukhanyan, T.; Sung, C.; Kumar, J.; Tripathy, S. K.; Samuelson, L.; Balogh, L.; Tomalia, D. A. (1999): Electrostatic Multilayer Deposition of a Gold-Dendrimer Nanocomposite, *Chem. Mater*, Vol. 11, pp. 3268-3274.

Herman, V.; Boenig, (1988): Fundamentals of Plasma Chemistry and Technology, Technomic Publishing Co., Lancaster, Pennsylvania, pp. 165-194.

Ho, D. L.; Briber, R. M.; Glinka, C. (2001): Characterization of organically Modified clay using scattering and Microscopy techniques, *J. Chem. Mater*, Vol. 13, pp. 1923-1931.

Inving, S. M. (1968): *Kodak Photoresist Seminor*, Vol. 2, pp.26.

Kim, D.; Kim, C. (2002): Etching Characteristics of $SrBi_2Ta_2O_9$ Thin Films in a Cl_2/CF_4/Ar Plasma, *Journal of the Korean Physical Society*, Vol. 41, pp. 439-444.

Kim, M. C.; Yang, S. H.; Boo, J. H.; Han, J. G. (2003): Surface treatment of metals using an atmospheric pressure plasma jet and their surface characteristics, *Surface and coatings Technology*, Vol. 174-175, pp. 839-844.

Koo, J. H.; Stretz, H.; Bray, A.; Wootan, W.; Mulich, S.; Powell, B.; Weispfenning, J.; Grupa, T. (2003): Nanostructured materials for Rocket Propulsion System, 44th AIAA/ASME/ASCE/AHS Structures, Structural Dynamics, and Materials Conference, Norfolk, VA, April 7-10, pp.1-11.

Lan, T.; Pinnavaia, T. J. (1994): Clay-Reinforced Epoxy Nanocomposites, *Chem. Mater*, Vol. 6, pp. 2216-2219.

Li, G. Z.; Wang, L.; Toghiani, H.; Daulton, T. L.; Koyama, K.; Pittman, C. U. Jr. (2001): Viscoelastic and Mechanical properties of Epoxy/Multifunctional Polyhedral Oligomeric Silsesquioxane Nanocomposites and Epoxy/Ladder like Polyphenylsilsesquioxane Blends, *Macromolecules*, Vol. 34, pp. 8686-8693.

Manias, E. (2001): Concurrent Enhancement of Various Material Properties in Polymer/Clay Nano composites in Advance Composites, Technomic Publishing Co., VA, editors: Hyer M.W, Loss A.C.

Marnor, M.; Auret, F. D.; Goodman, S. A.; Malherbe, J. B. (1999): Argon plasma sputter etching induced defect levels in strained, epitaxial p-type Si-Ge alloys, *Thin Solid Films*, Vol. 343-344, No. 4, pp. 416-419.

Mitra, Y.; Hossein, T.; Kingery, W. L.; Pittman, C. U. Jr. (2004): Preparation Characterization and properties of Exfoliated/Delaminated Organically Modified Clay/Dicyclopentadiene Resin Nanocomposites, *Macromolecules*, Vol. 37, pp. 2511-2518.

Morgan, A. B.; Gilman, J. W.; Jackson, C. L. (2002): Proceedings of the American Chemical Society: Polymeric Materials Science & Engineering, Vol. 82, San Francisco, CA, March 2000; American Chemical Society: Washington, DC, 2000, pp.270-271.

Patton, R. D.; Pittman, C. U. Jr.; Wang, L.; Hill, J. R. (1999): Vapor Grown Carbon Fiber Composites with Epoxy and Poly(phenylene sulfide) Matrices, *Composites, Part A*, Vol. 30, pp.1081-1091.

Percy, M. J.; Barthet, C.; Lobb, J. C.; Khan, M. A.; Lascelles, S. F.; Vamvakaki, M.; Armes, S. (2000): Synthesis and Characterization of Vinyl Polymer-Silica Colloidal Nanocomposite, *Langmuir*, Vol. 16, pp. 6913-6920.

Pyun, J.; Matyjaszewski, K.; Kowalewski, T.; Savin, D.; Patternson, G.; Kickelbick, G.; Huesing, N. (2001): Synthesis of Well-Defined Block Copolymers Tehered to Polysilsesquioxane Nanoparticle and their Nanoscale Morphology on Surfaces, *J. Am. Chem. Soc.*, Vol. 123, pp. 9445-9446.

Tamaki, R.; Choi, J.; Laine, R. M. (2003): Polyimide Nanocomposite from Octe Silsequioxane, *Chem. Mater*, Vol. 15, pp.739-797.

Yoshihara, M.; Oie, H.; Okada, A.; Matsui, H.; Ohshiro, S. (2002): Synthesis of Yttrium-Organic Hybrid Networks, *Macromolecules*, Vol. 35, pp. 2435-2436.